# Variable dimensionality in 'hollow' hybrid tin iodide perovskites

Jason A. McNulty, Alexandra M. Z. Slawin and Philip Lightfoot*[a]

[a]*School of Chemistry and EaStChem, University of St Andrews, Fife, KY16 9ST, UK. E-mail: pl@st-andrews.ac.uk*

## Supplementary Information

### Synthesis

Tin powder (~325 mesh, 99.8% metals basis), hydroiodic acid (HI, 57%, w/w aqueous solution stabilised with 1.5% HPA), hypophosphorous acid ($H_3PO_2$ (HPA), 50% w/w aqueous solution) and 1,2,4-triazole ($C_2H_3N_3$, 99%) were purchased from Alfa Aesar. All chemicals were directly used without further purification.

Both $(TzH)_{11}(H_3PO_2)Sn_6I_{23}$ and $(TzH)_xSn_2I_7$ were crystallised by a slow evaporation method.

For $(TzH)_{11}(H_3PO_2)Sn_6I_{23}$ $[C_2N_3H_4]_{11}[H_3PO_2]Sn_6I_{23}$: Tin powder (237 mg, 2 mmol) was dissolved in conc. HI (5 ml) and HPA (5 ml) with moderate heating. Once fully dissolved, 1,2,4-triazole (138 mg, 2 mmol) was added and the solution allowed to cool. After an hour orange/red crystals were obtained. These were filtered and washed with diethyl ether.

For $(TzH)_3Sn_2I_7$ $[C_2N_3H_4]_3Sn_2I_7$: The reaction mixture used in the synthesis of $(TzH)_{11}(H_3PO_2)Sn_6I_{23}$ was left for 2 months. Orange/red crystals were obtained. These were filtered and washed with diethyl ether. Elemental analysis: (Anal. Calc. (%) for $(TzH)_3Sn_2I_7$: C 5.39; N 9.44; H 0.91. Found: C 5.48; N 9.51; H 0.86).

The synthesis of both $(TzH)_{11}(H_3PO_2)Sn_6I_{23}$ and $(TzH)_3Sn_2I_7$ was carried out in air. HPA was used in the reaction to prevent oxidation of $Sn^{2+}$ to $Sn^{4+}$ while the crystals remained in solution. After filtration the crystals were stored under argon. In air both $(TzH)_{11}(H_3PO_2)Sn_6I_{23}$ and $(TzH)_3Sn_2I_7$ oxidise rapidly with a clear colour change and evolution of $I_2$.

### Characterisation

Single Crystal data were collected at 93 K and 173 K for $(TzH)_{11}(H_3PO_2)Sn_6I_{23}$ and $(TzH)_3Sn_2I_7$, respectively. Data were collected on a Rigaku Pilatus 200 K diffractometer using Mo-Kα radiation. Data were collected using CrystalClear (Rigaku).[1] Structures were solved by direct methods and refined using SHELX-2014[2] incorporated in the WINGX program.[3] Absorption corrections were performed semi-empirically from equivalent reflections on the basis of multi-scans.

In $(TzH)_{11}(H_3PO_2)Sn_6I_{23}$ non-H atoms were refined anisotropically and hydrogen atoms were treated as riding atoms. Due to the strong hydrogen bonding between $H_3PO_2$ and two $TzH^+$ cations these are both known to exhibit disorder over two positions around the pseudo two-fold axis and C/N positions have been assigned accordingly. For all other $TzH^+$ cations only the N with the lone pair could be assigned unambiguously and therefore all other C/N positions have been assigned as 50:50 occupancy to maintain the correct compositional formula. This model allows full anisotropic refinement of all $TzH^+$ moieties.

In $(TzH)_3Sn_2I_7$, only the tin iodide framework has been refined. Models with partial assignment of $TzH^+$ fragments were trialled, but no complete and satisfactory model could be obtained. The CHN analysis supports the formula proposed, with all $TzH^+$ moieties intact. Moreover, although some degradation of linear amines has been observed under similar reaction conditions, there is no evidence to suggest this would also take place with the cyclic, conjugated $TzH^+$ amine. Hence, we are confident of the formula proposed.

Preliminary UV-vis absorption was carried out on $(TzH)_{11}(H_3PO_2)Sn_6I_{23}$ using a JASCO-V550 ultraviolet-visible spectrophotometer with the wavelength range at 200 nm to 900 nm (JASCO Corporation, Essex, UK).

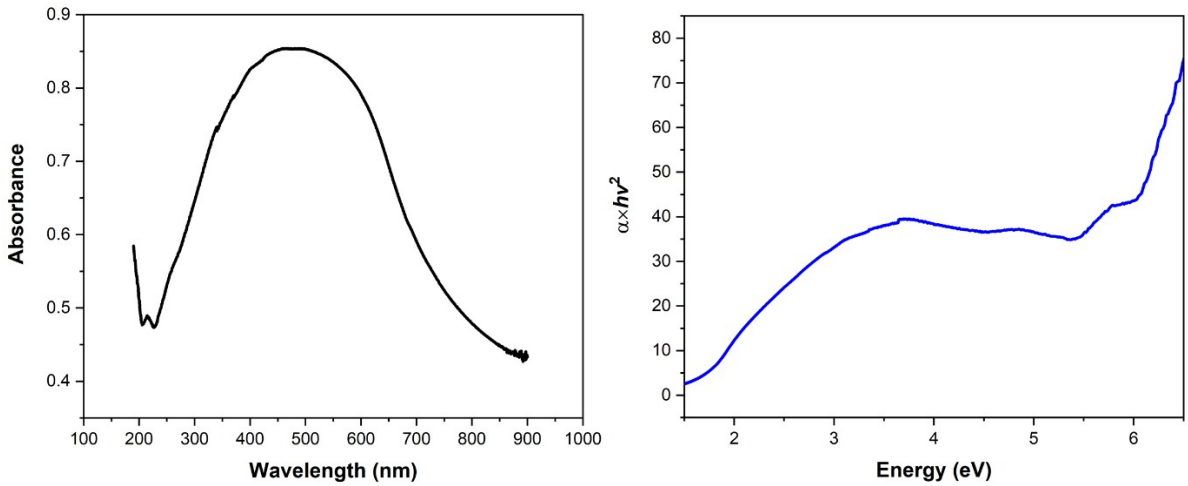


**Figure S1.** Preliminary UV-vis absorption spectra (left) and calculated Tauc plot (right) for $(TzH)_{11}(H_3PO_2)Sn_6I_{23}$ collected at room temperature.

The bond length distortion of the $SnI_6$ octahedra of both compositions was calculated using eq. 1,[4] where $d$ is the average Sn-I bond distance and $d_n$ are the six individual bond distances. The bond angle variance of each octahedron from the ideal 90° of an undistorted structure was calculated using eq. 2,[5] where $\theta_i$ is the individual I-Sn-I angle.

$$\Delta d = \left(\frac{1}{6}\right)\sum\left[\frac{d_n - d}{d}\right]^2 \quad \textbf{(1)}$$

$$\sigma^2 = \sum_{i=1}^{12}\frac{(\theta_i - 90)^2}{11} \quad \textbf{(2)}$$

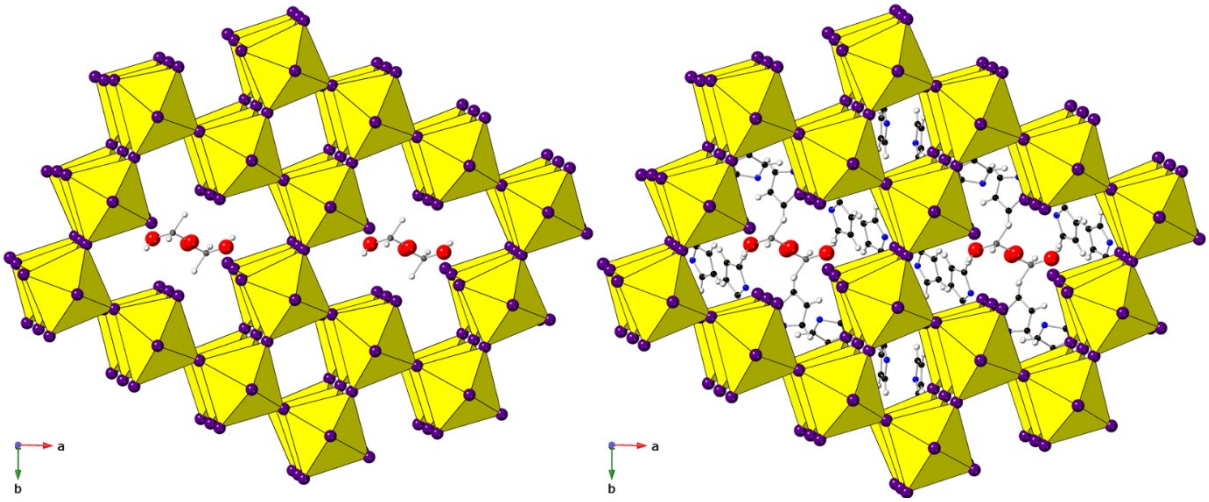


**Figure S2.** Crystal structure of $(TzH)_{11}(H_3PO_2)Sn_6I_{23}$ viewed along the *c*-axis highlighting the position of $H_3PO_2$ (left) and the surrounding amines in the inter-layer site (right). $H_3PO_2$ is positioned between triple perovskite-like blocks in the inter-layer site and below the 'hollow' channel caused by the B-site deficiency.

**Table S1** Selected bond lengths (Å) and angles (°) derived from single crystal data of $(TzH)_{11}(H_3PO_2)Sn_6I_{23}$ collected at 93 K. Bridging and terminal iodine atoms are denoted with *b* or *t*, respectively.

| **Sn-I** | | | | | | |
|---|---|---|---|---|---|---|
| | Sn1-I4$^t$ | 2.925(1) | Sn2-I7$^t$ | 2.981(1) | Sn3-I14$^t$ | 2.991(1) |
| | Sn1-I1$^t$ | 3.069(1) | Sn2-I11$^b$ | 3.026(1) | Sn3-I15$^b$ | 3.024(1) |
| | Sn1-I3$^b$ | 3.120(1) | Sn2-I10$^t$ | 3.115(1) | Sn3-I12$^t$ | 3.101(1) |
| | Sn1-I5$^b$ | 3.224(1) | Sn2-I5$^b$ | 3.207(1) | Sn3-I13$^b$ | 3.222(1) |
| | Sn1-I2$^b$ | 3.271(1) | Sn2-I9$^b$ | 3.312(1) | Sn3-I11$^b$ | 3.300(1) |
| | Sn1-I6$^b$ | 3.449(1) | Sn2-I8$^b$ | 3.365(1) | Sn3-I3$^b$ | 3.353(1) |
| **Sn-I** | Sn4-I18$^t$ | 2.887(1) | Sn5-I20$^t$ | 2.905(1) | Sn6-I24$^t$ | 2.952(1) |
| | Sn4-I16$^t$ | 3.097(1) | Sn5-I21$^b$ | 3.132(1) | Sn6-I22$^b$ | 3.047(1) |
| | Sn4-I6$^b$ | 3.170(1) | Sn5-I8$^b$ | 3.143(1) | Sn6-I2$^b$ | 3.081(1) |
| | Sn4-I9$^b$ | 3.223(1) | Sn5-I19$^b$ | 3.215(1) | Sn6-I13$^b$ | 3.191(1) |
| | Sn4-I17$^b$ | 3.267(1) | Sn5-I17$^b$ | 3.224(1) | Sn6-I23$^b$ | 3.264(1) |
| | Sn4-I15$^b$ | 3.619(1) | Sn5-I22$^b$ | 3.522(1) | Sn6-I21$^b$ | 3.398(1) |

| **I-Sn-I** | **Sn1** | **Sn2** | **Sn3** |
|---|---|---|---|
| | 84.92(4) | 83.49(4) | 82.41(4) |
| | 85.10(4) | 88.03(3) | 86.10(4) |
| | 85.68(4) | 88.04(4) | 87.82(4) |
| | 87.11(4) | 89.28(4) | 88.84(4) |
| | 88.24(4) | 90.07(4) | 88.90(4) |
| | 89.54(4) | 90.47(4) | 89.25(4) |
| | 91.01(4) | 90.58(4) | 90.61(4) |
| | 91.54(4) | 90.84(4) | 92.05(4) |
| | 92.28(4) | 90.88(4) | 92.10(4) |
| | 92.43(4) | 91.81(4) | 92.64(4) |
| | 95.49(4) | 92.73(4) | 92.68(4) |
| | 95.77(4) | 94.14(4) | 96.19(4) |

| **I-Sn-I** | **Sn4** | **Sn5** | **Sn6** |
|---|---|---|---|
| | 81.85(4) | 79.17(4) | 85.56(4) |
| | 83.65(4) | 84.16(4) | 86.06(4) |
| | 86.27(4) | 87.83(4) | 87.78(4) |
| | 88.04(4) | 87.99(4) | 88.33(4) |
| | 88.13(4) | 90.06(4) | 89.21(4) |
| | 88.16(4) | 90.48(4) | 89.52(4) |
| | 90.45(4) | 90.64(4) | 89.63(4) |
| | 91.17(4) | 91.21(4) | 90.35(4) |
| | 92.92(4) | 91.56(4) | 91.75(4) |
| | 94.26(4) | 91.81(4) | 92.66(4) |
| | 97.37(4) | 92.77(4) | 93.97(4) |
| | 97.66(4) | 102.66(4) | 95.10(4) |

| **Sn-I-Sn** |
|---|

| | | | | | | |
|---|---|---|---|---|---|---|
| | Sn1-I5-Sn2 | 170.57(4) | Sn1-I3-Sn3 | 174.29(4) | Sn1-I6-Sn4 | 166.26(4) |
| | Sn1-I2-Sn6 | 173.02(4) | Sn2-I11-Sn3 | 171.31(4) | Sn2-I9-Sn4 | 178.32(4) |
| | Sn2-I8-Sn5 | 173.31(4) | Sn3-I15-Sn4 | 174.37(4) | Sn3-I13-Sn6 | 171.49(4) |
| | Sn4-I17-Sn5 | 165.02(4) | Sn5-I19-Sn5 | 180 | Sn5-I21-Sn6 | 177.50(4) |
| | Sn5-I22-Sn6 | 175.30(4) | Sn6-I23-Sn6 | 180 | | |
| **BVS** | | | | | | |
| | Sn1 | 2.10 | Sn2 | 2.09 | Sn3 | 2.10 |
| | Sn4 | 2.04 | Sn5 | 2.06 | Sn6 | 2.17 |
| | $I1^{t}$ | 0.43 | $I2^{b}$ | 0.66 | $I3^{b}$ | 0.57 |
| | $I4^{t}$ | 0.63 | $I5^{b}$ | 0.57 | $I6^{b}$ | 0.47 |
| | $I7^{t}$ | 0.54 | $I8^{b}$ | 0.54 | $I9^{b}$ | 0.50 |
| | $I10^{t}$ | 0.38 | $I11^{b}$ | 0.70 | $I12^{t}$ | 0.39 |
| | $I13^{b}$ | 0.59 | $I14^{t}$ | 0.52 | $I15^{b}$ | 0.58 |
| | $I16^{t}$ | 0.39 | $I17^{b}$ | 0.53 | $I18^{t}$ | 0.69 |
| | $I19^{b}$ | 0.57 | $I20^{t}$ | 0.66 | $I21^{b}$ | 0.53 |
| | $I22^{b}$ | 0.58 | $I23^{b}$ | 0.50 | $I24^{t}$ | 0.58 |

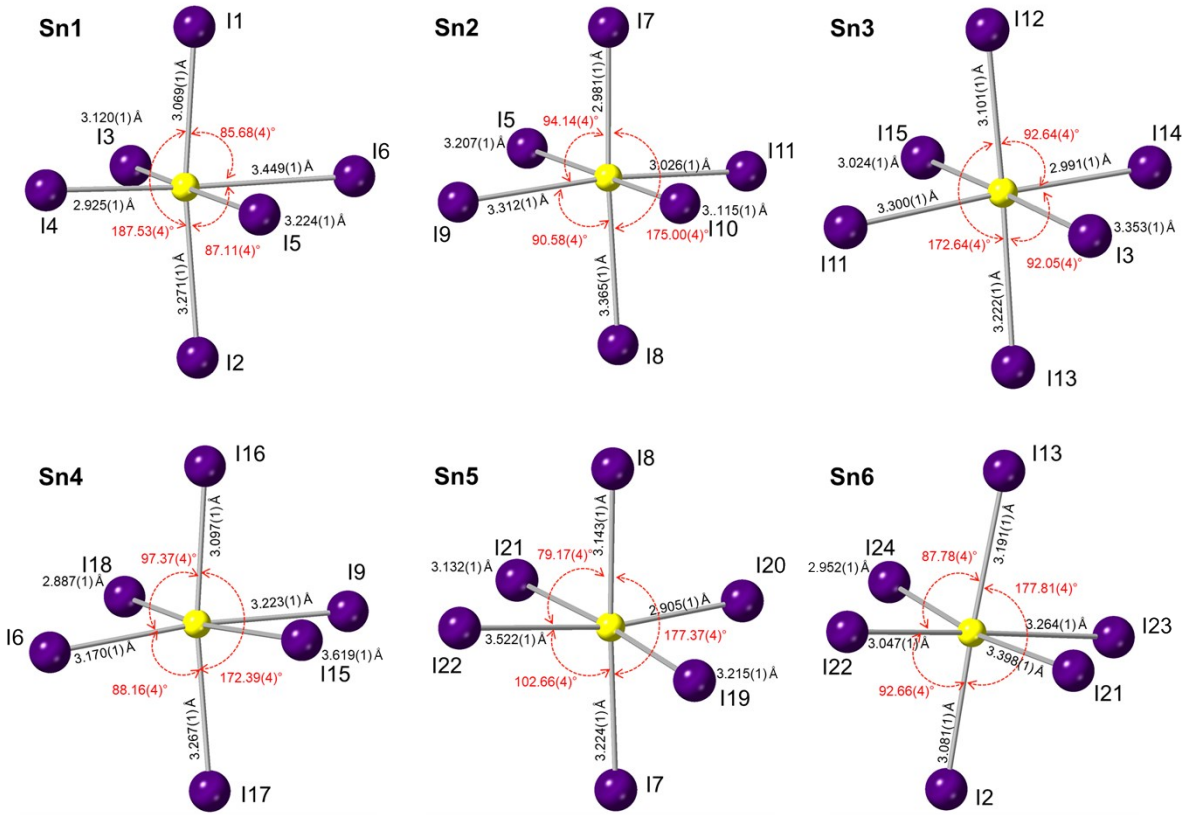


**Figure S3.** Ball and stick representations of the octahedra present in $(TzH)_{11}(H_3PO_2)Sn_6I_{23}$ at 93K highlighting the distortion in both bond lengths and bond angles.

**Table S2** Selected bond lengths (Å) and angles (°) derived from single crystal data of for $(TzH)_xSn_2I_7$ collected at 173 K.

| | **Sn1** | | **Sn2** | |
|---|---|---|---|---|
| **Sn-I** | | | | |
| | Sn1-I1 | 2.928(4) | Sn2-I5 | 2.961(3) |
| | Sn1-I3 | 3.096(4) | Sn2-I6 | 3.091(3) |
| | Sn1-I2 | 3.150(4) | Sn2-I4 | 3.201(5) |
| | Sn1-I2 | 3.255(4) | Sn2-I4 | 3.207(5) |
| | Sn1-I8 | 3.302(4) | Sn2-I7 | 3.283(4) |
| | Sn1-I6 | 3.499(4) | Sn2-I3 | 3.403(4) |
| **I-Sn-I** | | | | |
| | 84.43(10) | | 84.94(10) | |
| | 85.84(10) | | 86.42(10) | |
| | 87.58(10) | | 87.32(10) | |
| | 89.57(10) | | 87.44(10) | |
| | 90.16(10) | | 89.71(8) | |
| | 90.19(10) | | 90.99(10) | |
| | 90.86(10) | | 91.13(10) | |
| | 90.95(10) | | 91.39(10) | |
| | 91.92(8) | | 91.52(9) | |
| | 92.45(10) | | 92.09(9) | |
| | 92.98(10) | | 92.54(8) | |
| | 93.04(10) | | 94.17(10) | |
| **Sn-I-Sn** | | | | |
| | Sn1-I2-Sn1 | 177.35(10) | Sn1-I8-Sn1 | 180 |
| | Sn2-I4-Sn2 | 175.63(10) | Sn2-I7-Sn2 | 180 |
| | Sn1-I3-Sn2 | 176.71(10) | Sn1-I6-Sn2 | 174.40(10) |
| **BVS** | | | | |
| | Sn1 | 1.97 | Sn2 | 1.97 |
| | I1 | 0.62 | I2 | 0.60 |
| | I3 | 0.57 | I4 | 0.59 |
| | I5 | 0.57 | I6 | 0.53 |
| | I7 | 0.48 | I8 | 0.45 |

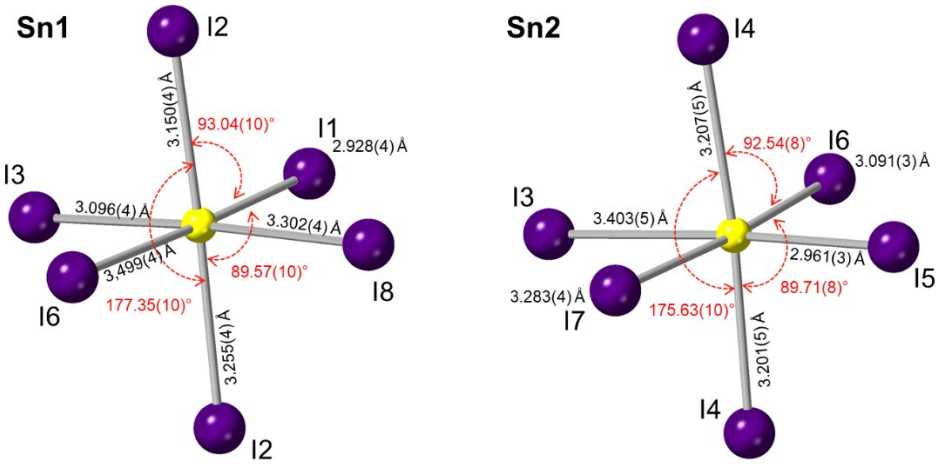


**Figure S4.** Ball and stick representations of the octahedra present in $(TzH)_xSn_2I_7$ at 173K highlighting the distortion in both bond lengths and bond angles.

**References**


1. Rigaku, 2014, *CrystalClear*, Rigaku Corporation, Tokyo, Japan.
2. G. M. Sheldrick, *Acta Crystallogr.*, 2015, **C71**, 3.
3. L. J. Farrugia, *J. Appl. Crystallogr.*, 2012, **45**, 849.
4. M. W. Lufaso and P. M. Woodward, *Acta Crystallogr.*, 2004, **B60**, 10.
5. K. Robinson, G. V. Gibbs and P. H. Ribbe, *Science*, 1971, **172**, 567.